Australian Government
Department of Defence
Defence Science and
Technology Organisation

Review of Solid Propellant Ignition Models Relative to the Interior Ballistic Modelling of Gun Systems

A. Harrland and I.A. Johnston

Weapons Systems Division

Defence Science and Technology Organisation

DSTO–TR–2735

ABSTRACT

The modelling of solid propellant ignition is investigated with the aim of implementation into the numerical code Casbar. The current state of the art in solid propellant ignition and combustion modelling is reviewed, with a simplified condensed phase ignition model chosen as the suitable candidate. A number of methods of solving the mathematical models are analysed, with results compared. Based on these results, the solution by integral methods to the condensed phase model was chosen for implementation into Casbar.

Published by

DSTO Defence Science and Technology Organisation
PO Box 1500
Edinburgh, South Australia 5111, Australia

Telephone: (08) 7389 5555
Facsimile: (08) 7389 6567

AR No. 015-373
August, 2012

APPROVED FOR PUBLIC RELEASE

Review of Solid Propellant Ignition Models Relative to the Interior Ballistic Modelling of Gun Systems

Executive Summary

Solid propellant ignition (and the evolution to self-sustained combustion) is a highly complex physicochemical process, involving the transition of a stable solid propellant state through to a luminous burning resulting from the application of heat energy [1]. For solid rocket and gun applications, ignition stimulus is usually in the form of a pyrotechnic igniter emitting heat energy and hot particles into the propellant bed. The action of simultaneous energy sources from convection of the hot gases, conduction from impingement of hot particles, radiation from both the hot igniter gases and particles, and even heat from atom recombination and vapour condensation, all act to ignite the propellant [2].

Interior ballistic modelling is used in a wide range of defence applications, and forms a key analytical tool for the assessment of gun and rocket propulsion systems. A range of phenomena occurring during the interior ballistics cycle are related to solid propellant ignition processes, therefore the accurate reproduction of ignition phenomena is important. Australia's Defence Science and Technology Organisation has capability in performing gun interior ballistics modelling through its numerical code, Casbar. Casbar solves the governing equations for the transient flow of chemically reacting gas and particulates within a finite volume discretisation of the computational domain [3].

Currently in Casbar propellant ignition is modelled using a simple go/no-go condition, whereby if the gas surrounding the propellant is above the defined propellant ignition temperature, the grain will combust. This ignition criterion does not account for finite-rate grain heating and the experimentally observed ignition delay of solid propellant grains, and thus generally predicts an unrealistically fast propellant ignition.

This report describes the solid propellant ignition and combustion phenomena, and investigates a number of ignition models suitable for implementation into the Casbar code. The three main areas of ignition models (solid-phase, heterogeneous and gas-phase reactions models) encompass a broad range of complexity and numerical efficiency. It is desirable to choose a model that is accurate, while being flexible. Ultimately, the solid-phase ignition model was chosen for implementation in Casbar.

A number of numerical techniques for solution of the solid-phase ignition model were reviewed. In numerical modelling it is required that the solution of the model be adequately robust, while reducing the impact on the simulation time. In all of the investigated heat flux scenarios, the integral method was able to adequately approximate the final ignition time to within an acceptable level of accuracy (in comparison to the finite difference approximation). Situations involving highly variable heat fluxes were employed to test the applicability of the integral method. These scenarios were constructed to accentuate the variability of the heat flux, and situations like this are not expected in typical interior ballistic simulations. The integral method is therefore considered an appropriate candidate for implementation in Casbar.

THIS PAGE IS INTENTIONALLY BLANK

Contents

Figures

Glossary

A Area, m^2; Burn-rate law pre-exponential, $^m/_s \cdot MPa^n$

c_p Constant pressure specific heat capacity, $^J/_{kg \cdot K}$

c_v Constant volume specific heat capacity, $^J/_{kg \cdot K}$

D_i Diffusion coefficient, $^{m^2}/_s$

D_p Effective grain diameter, m

D_{T_i} Thermodiffusion coefficient, K^{-1}

E_A Activation energy, $^J/_{mol}$

f Frequency factor

F_s Safety factor

h Heat transfer coefficient, $^W/_{m^2 \cdot K}$; intensive enthalpy, $^J/_{kg}$

k Thermal conductivity, $^W/_{m \cdot K}$

m Mass, kg

Nu Nusselt number

p Pressure, Pa; Order of convergence

q Heat flux, $^J/_{m^2}$

$\dot{q}$ Rate of heat flux, $^W/_{m^2}$

Q Heat source, $^W/_{kg}$

$\dot{Q}$ Rate of heat evolution, $^W/_{m^3}$

$\dot{Q}_r$ Rate of reaction heat evolution, $^W/_{m^3}$

r Linear regression, m

$\dot{r}$ Linear regression rate, $^m/_s$

R Universal gas constant, $^J/_{mol \cdot K}$

Re Reynolds number

t Time, s

T Temperature, K

u Velocity, $^m/_s$

V_p Propellant grain volume, m^3

x Spatial co-ordinate, m

y Spatial co-ordinate, m

Y Species mass fraction

Greek symbols

α Thermal diffusivity, $^{m^2}/_{s}$

β Absorptivity, m^{-1}

γ Ratio of specific heats

δ Penetration distance, m

ϵ Emissivity

μ Dynamic viscosity, $Pa \cdot s$

π Pi, 3.14159

ρ Density, kg/m^3

σ Stefan-Boltzmann constant, 5.670×10^{-8} $^{W}/_{m^{-2}K^{-4}}$

ϕ Energy flux, $^{W}/_{m^2 \cdot s}$; voidage fraction

Subscript

A Activation

cond Conductive heat transfer

conv Convective heat transfer

f Mass averaged quantity within foam layer

g Gas phase

i Propellant/gas interface; Spatial discretization position

ign Ignition

∞ Value at a large distance away from the area of interest

l Liquid phase

rad Radiative heat transfer

s Solid phase

surf Surface

Superscript

n Temporal discretization position

THIS PAGE IS INTENTIONALLY BLANK

1 Introduction

The accurate reproduction of ignition phenomena is an important aspect of interior ballistic modelling. A range of phenomena occurring during the interior ballistics cycle are related to solid propellant ignition processes. Australia's Defence Science and Technology Organisation currently has capability in performing gun interior ballistics modelling through its code, Casbar. Casbar solves the governing equations for the transient flow of chemically reacting gas and particulates within a finite volume discretisation of the computational domain [3]. Currently propellant ignition is modelled using a simple go/no-go condition, whereby if the gas surrounding the propellant is above the defined propellant ignition temperature, the grain will combust. This ignition criterion does not account for finite-rate grain heating and the experimentally observed ignition delay of solid propellant grains, and thus generally predicts an unrealistically fast propellant ignition. This report describes the solid propellant ignition and combustion phenomena, and investigates a number of ignition models suitable for implementation into the Casbar code.

1.1 Solid propellant ignition and combustion

Solid propellant ignition (and the evolution to self-sustained combustion) is a highly complex physicochemical process, involving the transition of a stable solid propellant state through to a luminous burning resulting from the application of heat energy [1]. For solid rocket and gun applications, ignition stimulus is usually in the form of a pyrotechnic igniter emitting heat energy and hot particles into the propellant bed. The action of simultaneous energy sources from convection of the hot gases, conduction from impingement of hot particles, radiation from both the hot igniter gases and particles, and even heat from atom recombination and vapour condensation, all act to ignite the propellant [2].

Gun and rocket propellants traditionally comprise several chemical ingredients combined either heterogeneously or homogeneously to form the solid [4]. The chemical ingredients, which can consist of oxidizer, fuel, binder, plasticiser, curing agent, stabilizer, bonding agent, burning rate catalyst, anti-aging catalyst, opacifier, flame suppressant, combustion instability suppressant and cross-linking agent [5] are either connected on a microscopic level (homogeneous) or mixed on a macroscopic level (heterogeneous) to form the desired physical and chemical properties of the propellant. The ignition and combustion processes for homogeneous and heterogeneous propellants possess many subtle differences between formulations and ingredients, however the underlying physical mechanisms are similar. Traditionally, homogeneous propellants (such as single base nitrocellulose or double base nitrocellulose and nitroglycerine) are employed in gun propellants, while heterogeneous (such as AP, HMX or RDX) propellants are more often employed in solid rocket propellants. Composite propellants are finding more use in gun propellant applications in recent times [6], however AP based propellants are not used in gun applications due to the large amount of hydrogen chloride (HCl) produced in the combustion products, which acts to accelerate gun barrel erosion [7].

Many complex processes occur between the initial application of heat energy and steady state combustion; solid propellants are converted to gas products through oxidation at extremely high pressures and temperatures in the order of a few thousand Kelvin can be

reached. All of this occurs over a fraction of a second, resulting in an extremely hostile environment that is still not completely understood, despite decades of research [8]. Significant condensed phase reactions, coupled with a large number of gas phase reactions, compound the difficulties of forming a suitable model of solid propellant ignition and combustion.

When a propellant is subjected to sufficient heat energy such that self-sustained combustion is obtained, three significant reaction regions develop defined by the thermal state of the propellants (or its constituents), as shown in Figure 1. The solid (or condensed) phase region is the furthest from the source of heat energy, and consists of the propellant in its initial solid state. Upon the external application of heat the surface temperature begins to increase in conjunction with heat being conducted away from the surface into the solid core. The surface temperature continues to increase until the point of phase change is reached. Solid-phase exothermic reactions may occur in some propellant ingredients (such as AP [9] or ADN [4]) leading to thermal degradation within the solid phase, however these are typically insignificant and often neglected. The second region can generally be considered to consist of either a two-phase mixture of melted liquid propellant and evaporated propellant gas or an infinitesimally small sublimation interface. Some propellants exhibit melting behaviour while others do not [10], in which the melt layer can be formulated with sublimation or pyrolysis mechanisms for transition to the gas phase [11]. Although the melt line is often represented as a sharp discontinuity in theoretical models, in reality it is a blurred region consisting of a slurry of solid and liquid propellant. There is no definite distinction between regions, and complex reactions such as vaporization, condensation, decomposition and oxidation can all occur. This layer is often referred to as the foam layer due to its 'frothy' nature [7]. The final region in the combustion process is the gas-phase layer, a region where the evaporated species react and decompose into other species.

The gas layer itself has transient, pressure dependent behaviour that can consist of multiple sub-layers. At low burning pressures (below approximately 1 MPa) there is no visible flame above the burning surface of the propellant. As the pressure increases, a weak flame is sometimes visible above the burning surface. As the pressure increases further, the flame moves closer to the propellant surface, until pressures of around 10MPa, where it appears attached to the propellant burning surface [10]. The region between the burning surface and visible flame can consist of two regions, labelled the fizz zone and the dark zone. Within both these regions, the gas temperature is relatively constant due to a slow reduction of NO to N_2 [10]. Rapid reactions occur in the fizz zone just above the propellant surface. Within the dark zone the oxidised products released from the fizz zone react relatively slowly, and the zone is only present if the pressure and temperature are sufficient [7]. Within the flame zone, the oxidation reactions release large amounts of energy with the final temperature approaching the adiabatic flame temperature of the propellant. The heat feedback from the flame in the form of radiation, convection and conduction sustains the reactions until the solid propellant is consumed. Flame stand-off plays a critical role in the amount of heat feedback to the propellant.

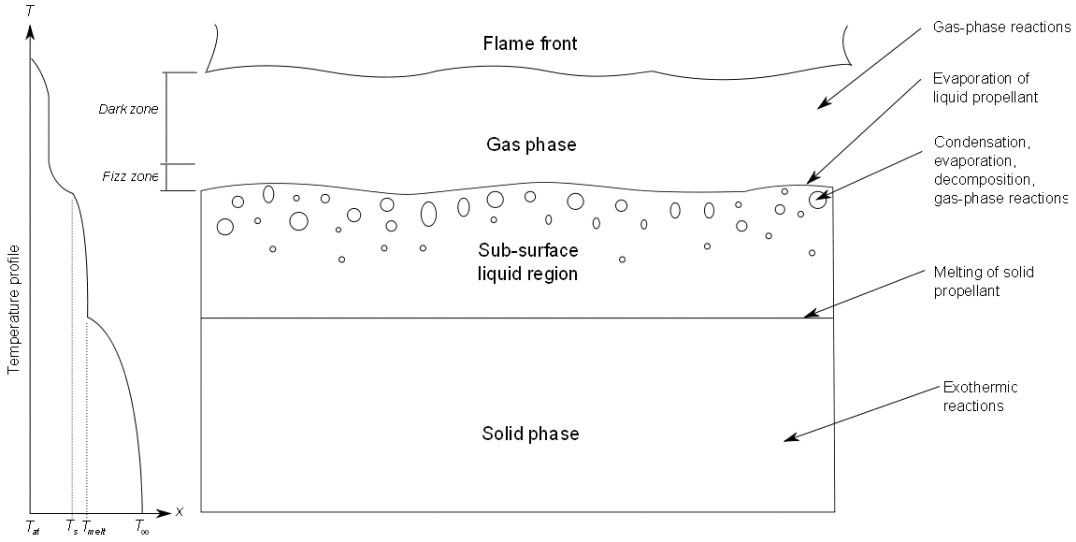

Figure 1: *Solid propellant combustion schematic (adpated from [4]).*

2 Current state of solid propellant ignition and combustion modelling

Propellant ignition modelling has been an area of research since the 1950s, with many different theoretical models developed [5]. Propellant ignition models can be catagorized into three main types: solid-phase (reactive solid), heterogeneous, and gas phase reaction models [4].

Solid phase reaction models were the first developed, and are generally the least complicated due to the extensive simplifications employed [12]. The internal energy of the propellant, often coupled to a single-step Arrhenius reaction within the condensed phase, is considered the dominant driving force of ignition. The effects of gas phase reactions are assumed to not influence the time to ignition, and therefore neglected.

Heterogeneous ignition models were the next form of ignition model developed, due to experimental observations of ignition from introduced hypergolic oxidizer gases [13]. These models allow for observed behaviour of composite propellants by including the diffusion of fuel and oxidizer species at the propellant surface. The complexity of the system is increased over the simple condensed phase models through the tracking of species concentration at the solid-gas interface. Heterogeneous ignition models are based on the assumption that surface interface reactions are the driving force for ignition. The gas phase is assumed to consist of products from the combustion process.

The third type of solid propellant ignition/combustion model is the gas phase model. Gas phase models increase the complexity over heterogeneous models by incorporating the reactions and species concentration within the gas phase. The gas phase reactions are considered to be the driving factor towards ignition, with the condensed phase contributions to species decomposition generally neglected. The gas phase models have the ability to treat the entire ignition transient from heat addition to the stable solid right through to pressure-dependent steady-state combustion of the propellant. Some models may be used to predict the burn rate characteristics of composite propellants, however these are still in their infancy and rely heavily on empirical results [8]. This section gives an overview of the research into solid propellant ignition and combustion models from the early solid phase models, through to the current multi-species gas phase models.

2.1 Solid-phase (reactive solid) ignition models

Solid phase ignition models began as an extension of the solid phase thermal explosion theory. Hicks [12] developed a physical model of the homogeneous solid propellant ignition process, with no diffusion or consumption of propellant, and no chain reactions. The model is assumed to be one-dimensional, with the heat penetration only occurring over a fraction of the solid propellant depth for rapid application of heat. This assumption has been validated, with the thermal penetration depth observed to be in the order of $100\mu m$ at solid rocket motor operating pressures [4]. Although solid rocket motor operating pressures are significantly lower than typical gun systems, during the ignition phases the pressure within the gun chamber is often well below solid rocket motor operating pressures. The one-dimensional heat conduction equation states that the rate of energy accumulation

within the solid is equal to the rate of energy conduction plus the energy production due to solid phase exothermic reactions. This is therefore expressed in partial differential form as

$$\rho c_v \frac{\partial T}{\partial t} = k \frac{\partial^2 T}{\partial x^2} + \dot{Q} \tag{1}$$

$\dot{Q}$ is the rate of heat evolution per unit volume due to solid phase reactions, assumed to be of zero order and independent of species concentration, giving

$$\dot{Q} = \dot{Q}_r f e^{-E_A/R \cdot T} \tag{2}$$

where $\dot{Q}_r$ is the heat of reaction per unit volume (W/m^3). Boundary conditions were formulated based on the assumption that all important physical processes occur within the solid propellant. It is assumed that the thermal wave penetration is small, such that the temperature of the propellant at a relatively large distance into the grain is always equal to the initial temperature of the propellant, T_0. This assumption holds true if the time between heating and ignition is less than the time for the thermal wave to penetrate through the solid. This is valid for most gun applications, where high heating rates are applied over short time scales. If this is not the case, the boundary condition of zero temperature gradient at the propellant centre can be applied. At the solid/gas boundary, the heat flux is taken as the heat feedback from the gas to the solid phase, such that

$$k \frac{\partial T}{\partial x}|_{x=0} = \dot{q}\,(t) \tag{3}$$

The resulting system of equations was solved by neglecting solid phase reactions ($\dot{Q} = 0$) and transforming the variables to non-dimensional form.

Price *et al.* [14] considered the ignition of solid propellant under the influence of a laser, extending the model to accommodate the depletion of the solid material at a surface regression rate $\dot{r}$. Optical absorption of the laser energy due to transparency of the propellant within the energy equation for the solid phase was also included. The solid phase reaction partial differential equation (PDE) was therefore extended to

$$\rho c_v \frac{\partial T}{\partial t} = k \frac{\partial^2 T}{\partial x^2} + \rho c_v \dot{r} \frac{\partial T}{\partial x} + \beta \dot{q} e^{-\beta x} + \dot{Q} \tag{4}$$

where β is the absorptivity of the laser energy into the solid propellant (m^{-1}) and $\dot{q}$ is the energy flux per unit area from the laser ignition source ($W/m^{2} \cdot s$). The boundary conditions are similar to the previous model, however an updated heat balance at the moving boundary is introduced,

$$\dot{q}_i + \rho \dot{r} Q_s = k \frac{\partial T}{\partial x} \tag{5}$$

where $\dot{q}_i$ is the rate of heat transferred to the interface and Q_s is the heat source associated with the interface (which includes both chemical reactions and phase change).

The boundary condition at $x = \infty$ can be either taken as a fixed temperature (as per the original model) or, if condensed phase reactions are present, as zero gradient. Although an increase in the realism of the model over the original condensed phase model, considerable simplifications were required to form a tractable solution [14]. The thermophysical properties (such as ρ, c_v, k, β and Q_s) are assumed to be constant and therefore do not vary with time, temperature, pressure or propellant composition uniformity and optical properties. The assumption of single step, global Arrhenius rate equation for solid phase reactions is also a substantial simplification of the highly complex physicochemical process occurring. Even to the current day, the solid phase reactions are still not well understood [4].

Baer and Ryan [15] have further extended the solid phase analysis to include the transition from ignition to steady state regression, as opposed to a simple go/no-go condition. A relationship for the transition is produced by the consideration of an energy balance at the surface of the solid propellant. In their ignition model, the regression of the solid propellant surface under a known heat flux is taken into consideration, and is a function of surface temperature. A one-dimensional heat conduction equation neglecting condensed phase reactions is produced for dimensionless variables;

$$\frac{\partial \hat{T}}{\partial \hat{t}} - \hat{\dot{r}} \frac{\partial \hat{T}}{\partial \hat{x}} = \frac{\partial^2 \hat{T}}{\partial \hat{x^2}} \tag{6}$$

The heat feedback $\hat{\dot{q}}$ to the solid surface is assumed to occur from a single chemical reaction at (or near) the propellant surface. This feedback is related to the heat flux in the solid and the regression rate, given by

$$\hat{\dot{q}} = \hat{\dot{q}}_s + \hat{\dot{r}} \cdot \hat{Q} \tag{7}$$

where $\hat{\dot{q}}_s$ is the dimensionless heat flux just below the solid surface and $\hat{\dot{r}}$ is the dimensionless rate of gasification. Under steady-state regression, the dimensionless heat flux just below the surface is related to the difference between the steady-state regression temperature and the solid initial temperature, multiplied by the linear regression rate. For large values of the steady state regression temperature, the heat feed back to the solid surface is approximately related to pressure by an exponential factor. During the early ignition stages (when the surface temperature is much lower than during steady-state regression), the surface temperature is assumed to be dependent on the rate of generation of the reactive species from the solid phase. To approximate the transition from a kinetically limited condition to a diffusion-limited case, the following relationship is established

$$\frac{1}{\hat{\dot{q}}} = \frac{1}{\hat{\dot{q}}_a \hat{p}^n} + \frac{1}{e^{-1/\hat{T}_s}} \tag{8}$$

where $\hat{\dot{q}}_a$ is the dimensionless heat feedback at 1 atm and n is the pressure exponent for steady state feedback flux. The heat flux is then used to calculate the solid temperature profile through a Neumann boundary condition. This model is not justified theoretically by the authors, it is employed because it simply produces the correct asymptotes as the surface temperature is varied, while providing a smooth transition between the two rates.

Perez *et al.* [16] established a model for the initial pressure rise to steady state combustion (starting transient) of solid propellant rocket motors with high internal gas velocities, with comparison of their model with experimental data. The one dimensional heat conduction equation was solved for the solid propellant assuming the thermal wave penetration depth was negligible. The heat transfer to the propellant surface was calculated based on a local convective heat transfer coefficient. A third-degree polynomial solution for the propellant surface temperature was obtained through an integral method [17], which was then employed to calculate the surface temperature. The propellant was considered ignited when the surface temperature was above a specific, empirically derived value.

2.2 Heterogeneous ignition models

Heterogeneous reaction models were born from the experimental observations of the ignition of solid propellants subject to highly energetic oxidising gas environments via surface reactions at the solid/gas interface [18]. This theory is centered around exothermic surface reactions supplying the energy for stable combustion, and should not be confused with only applying to the heterogeneous nature of composite propellants [19]. In these models, the rate driving reaction was assumed to occur at the interface of the solid propellant and the oxidising gas. Diffusion between the decomposed solid propellant gasses and the oxidizer provided the fuel to initiate and sustain combustion. Williams [20] analyzes the ignition of a solid propellant through heterogeneous reactions. Similar to the homogeneous solid propellant models, a one-dimensional time dependent system is produced that involves the reaction between the solid propellant and an oxidising gas at the solid/gas interface. A known heat flux is introduced, which is absorbed at the solid/gas interface. Heat conduction is allowed to occur in both the solid and gas phases, however no phase change is accounted for. Condensed phase reactions are also neglected, however a single step Arrhenius reaction at the interface is present. Ignition is said to occur when the interface temperature reaches a certain value. A set of conservation equations is produced for the solid, gas and interface regions. For the solid and gas phases, the conservation of energy equation for both phases is

$$\frac{\partial h}{\partial t} = \frac{\partial \left(a \cdot {}^{\partial h}/_{\partial \psi} \right)}{\partial \psi} \tag{9}$$

where $a = \rho \cdot {}^{k}/_{c_p}$ and ψ is the stream function $\psi = \int_0^x \rho dx$. The conservation of energy condition at the solid/gas interface ($\psi = 0$) is written as

$$a_s \frac{\partial h_s}{\partial \psi} - a_g \frac{\partial h_g}{\partial \psi} = a_i \frac{\partial h_i}{\partial \psi} + q \tag{10}$$

with the Arrhenius rate equation at the interface given as

$$a_i \frac{\partial h_i}{\partial \psi} = QBf \left(Y_0 + {}^{h_i}/_{Q} \right) e^{-\mathrm{T_A}/\left(\mathrm{T_0 + h_g/c_{v_g}} \right)} \tag{11}$$

where B is a pre-exponential rate factor, Q the constant heat released in the surface reaction (per unit mass), and f is a function that expresses the dependence of the reaction

on the concentration of the oxidizing agent in the gas phase. Williams [20] approximates this as $f(Y) = Y^n$, where n is the order of the reaction. A Laplace transform is then used to solve the PDEs.

2.3 Gas-phase reaction ignition models

Gas phase models generally consider all (or most) of the physical mechanisms occurring during propellant combustion, thereby forming a complete mathematical description of the process. Beckstead *et al.* [4] have produced a very detailed review of the gas phase reaction model, with a summary of the physical processes reproduced here. As with all of the models, simplifications may be included to reduce the complexity of the system to be solved.

The solid phase region is modelled in a similar fashion to that described within Section 2.1, with the conservation of energy considered. In the case of propellant mixtures, the properties are taken as mass fraction averages of the constituents. The solid-phase exothermic reactions are not considered to contribute significantly to the ignition transient, and hence are neglected.

External to the solid phase region is the two-phase subsurface region, which consists of melted liquid propellant and evaporated propellant gas. Within this region there are a large number of complicated physicochemical processes occurring, which significantly increase the complexity of the system. Thermal decomposition, evaporation, bubble formation, gas-phase reactions within bubbles and transport of mass and energy between phases are all known to occur. One technique of simplifying the highly complex fluid dynamic interactions within the subsurface region is to employ a spatial averaging technique [4]. A fractional-voidage ϕ_f is used to define the cross sectional areas assumed by the gas phase and the condensed phase, assuming the bubbles are small and well dispersed. The area given by the gas bubbles is therefore

$$A_g = \phi_f A$$

where A_g is the cross sectional area of the propellant gas bubbles and A is the cross sectional area of the propellant sample. The integral form of the conservation equations are then combined using the fractional voidage. Species, mass and energy conservation equations are developed for the liquid and gas phases. Within the subsurface region both evaporation and condensation are occurring simultaneously. The net difference between the condensation and evaporation rates is determined through empirical means [21]. The mass conversion rate due to evaporation is then determined by multiplying the net mass conversion rate by the specific surface area, an empirically derived relationship between the number of bubbles and the fractional voidage.

The gas phase analysis is centred around the conservation of mass, energy and species transport for a multi-component chemically reacting system [4]. The system of equations allows for the accommodation of finite-rate chemical kinetics and variable thermophysical properties. A multi-phase treatment similar to the subsurface region can be employed when the gas phase contains dispersed condensed phase species. All thermophysical properties

are mass-averaged, and mass diffusion velocity V_i of an individual specie arises from both concentration and temperature gradients, given by

$$V_i = -D_i \frac{1}{X_i} \frac{\partial X_i}{\partial x} + D_i \frac{D_{T_i}}{X_i} \frac{1}{T} \frac{\partial T_g}{\partial x}$$

To close the system of equations the ideal gas law for a multi-component system is used, coupled with suitable boundary conditions to describe the energy and mass conversion occurring at the region interfaces.

As the gas phase reaction model is the most detailed of the models examined, with both the solid and gas phase considered, a simplified formulation is highly desirable. The solid phase conservation of energy equation is formulated considering surface regression;

$$\rho_s c_s \frac{\partial T_s}{\partial t} + \rho_s \dot{r} c_s \frac{\partial T_s}{\partial x} = k_s \frac{\partial^2 T_s}{\partial x^2}$$

however the boundary condition at the propellant surface is updated to include the energy associated with the change of phase from solid to gas. This gives the boundary condition at $x = 0$ as

$$-k_s \frac{\partial T_s}{\partial x} = \dot{q}\,(t) + \rho_s \dot{r} \dot{q}_{l-g}$$

where $\dot{q}_{l-g}$ is the heat associated with phase change. The sub-surface region is assumed to be infinitely thin and only occur in the interface between the solid and gas regions. Conservation of mass within the solid phase (assuming a single component system) is given by

$$\dot{m}_s = \rho_s \dot{r}$$

which simply states that the rate of change of mass within the solid phase is due to the regression of the propellant surface, multiplied by the density. A mass balance between the solid and gas phase yields the conservation of mass equation for the gas phase,

$$\dot{m}_g = \rho_g u_g = \dot{m}_s = \rho_s \dot{r}_s$$

Hence, the rate of mass addition into the gas phase is equal to the mass loss from the solid phase due to evaporation or sublimation. At the propellant surface, an equation is required that describes the phase change process to determine the rate of regression, $\dot{r}$. A number of models have been produced that give an approximation to the mass transfer between the phases covering a broad range of complexity. The decomposition of the solid has been approximated through the inclusion of a pressure dependence on surface regression [22]. The rate of regression of the solid propellant surface is given by

$$\dot{r} = \begin{cases} A p^n e^{\left(-E_A/R\left(\frac{1}{T_{ign}} - \frac{1}{T_{surf}}\right)\right)}; & T_{surf} < T_{ign} \\ A p^n; & T_{surf} = T_{ign} \end{cases}$$

where E_A is the activation energy for the pyrolysis equation. This model provides a smooth transition from the non-combusting decomposition to the steady state burning condition.

The conservation of energy equation for the gas phase is similar to the solid phase, and is given by

$$\rho_g c_g \frac{\partial T_g}{\partial t} + \rho_c \dot{r} c_g \frac{\partial T_g}{\partial x} = k_g \frac{\partial^2 T_g}{\partial x^2} + \dot{q}_g \dot{w}_g (x)$$

where $\dot{q}_g$ represents the heat released and $\dot{w}_g$ is the mass of reactant produced by the gas chemical reactions. Single or multiple specie kinetic mechanisms can be considered. Casbar currently has the provision for multi-component gas phase reactions, allowing complex gas kinetics of propellant combustion to be modelled. Arrhenius rate equations are used for the intermediate reaction steps. The boundary condition applied to the gas region is

$$T_{x=0} = T_{surf}$$

where T_{surf} is the propellant surface temperature. The gas temperature, and therefore resulting heat feedback to the propellant surface, is determined through the chemical kinetic model and the conservation equations for the gas phase. In this model, propellant ignition is assumed to have occurred when the heat feedback to the propellant surface is able to sustain the combustion without external influence however this definition is somewhat arbitrary as there is no definitive "ignition" point.

2.4 Defining the point of ignition

The establishment of deflagration within solid propellant is difficult to define, making the specification of the point of ignition somewhat vague. Ignition can be considered to have occurred when, upon the removal of the ignition stimuli, the propellant is able to achieve self-sustained combustion with no further application of energy [14]. From a modelling perspective, it is only important to have a distinct ignition criteria if the ignition and combustion models are separate (for example if Vieille's law is employed for pressure-dependant burning). For gas-phase reaction models defining an ignition point is somewhat arbitrary, as they are capable of modelling the transition from a solid propellant at ambient conditions right through to steady state combustion.

Just as there is a wide range of theories regarding propellant ignition, there are also many different methods for determining whether propellant ignition has occurred in both experimental and numerical investigations [19]. In experimental investigations, often propellant ignition is established by light emission, pressure and/or temperature rise, behaviour of the propellant after the removal of ignition stimuli or examination of the propellant grain after quenching. In mathematical investigations, typically ignition is defined to have occurred when a certain surface temperature has been reached (the ignition temperature), the rate of temperature rise is above a specified value, the rate of heat generation is greater than the rate of heat loss to the surroundings or by observation of the behaviour of the mathematical model after the artificial ignition stimuli has been removed. It is

important to select an ignition criterion not only relevant to the process being modelled, but also the ignition model itself.

2.5 Ignition model summary

The Casbar code was developed for the investigation of the interior ballistics of gun systems. As such, investigation of the intricate behaviour of propellant ignition and combustion on the micro-scale was not a design goal. The user is assumed to be interested in the macroscopic behaviour of interior ballistic arrangements, with the highest level of accuracy achievable with the minimum computational expense. A "fit for purpose" philosophy dictates that complex physical models that penalise the performance of the code through excessive memory storage or significantly increased numerical operations should only be included when they contribute to a significant increase in accuracy of the results of interest.

It is for this reason in the context of Casbar, a decision has been made not to pursue the gas phase reaction model further at this stage, due to both the increased complexity and the lack of physical data for real gun propellants. The most significant reason is the lack of physicochemical data available on specific solid propellants, without which accurate modelling cannot be undertaken. Some thermodynamic data have been published in the open literature ([23] for example), however the number of propellant formulations covered is limited. It is possible to establish a database of the required information for propellants of interest to DSTO, however these tests would be required to be performed for each new formulation to render the database accurate and up-to-date. Kinetic reaction rate data are much more elusive, and difficult to determine. To develop reaction rates for the solid propellants of interest for implementation into such a model would be a significant effort, and as such is not currently being pursued. Additionally the computational expense will be greater than simpler models, reducing the performance of the interior ballistic code. For these reasons the solid phase reaction model has been chosen for implementation into Casbar.

3 Numerical solution to the solid propellant ignition problem

This section outlines the numerical methods of solution to the solid propellant ignition models under investigation for use in Casbar. Three models of differing complexity are investigated to determine the most suitable model. The models can be considered solid-phase, all chosen due to their relative simplicity in comparison to gas-phase combustion models and their lack of requirement for reaction kinetics in relation to both heterogeneous and gas phase reaction models. Diffusion from the oxidizer into the propellant at the burning surface or within the gas phase is not considered to be a rate-affecting process. In addition, only one dimensional models are considered. Previously it has been stated that the burning rate of heterogeneous propellants is strongly dependent on the particle size of the oxidizer [10], and in such cases a one dimensional approximation would not be appropriate. The majority of propellants considered in Casbar are homogeneous single- and double-base gun propellants, with little variation with respect to composition within the grain.

Two numerical approaches to solve the resulting one dimensional solid phase ignition model have been investigated. The integral method is compared to a solution by finite differences, with results analysed to determine which solution would be implemented into Casbar.

3.1 Solution through integral methods

A relatively simple method for solving the one dimensional heat conduction equation within the solid phase involves using the integral method [17]. Using this method, the heat penetration into the solid propellant grain is assumed to follow a prescribed profile, and is dependant on the time history of the associated heat flux, and the instantaneous heat flux onto the propellant surface. Once the propellant surface temperature reaches the defined ignition temperature, the grain is assumed to ignite and allowed to burn following Vieille's pressure-dependant burning law. This method is the most commonly used in interior ballistic codes (eg. [24], [25], [26] and [27]).

The one dimensional heat conduction equation is significantly reduced in complexity to facilitate the solution. By the assumptions that all solid-phase thermodynamic properties do not vary with time or spatial position, that solid phase reactions are negligible, and there is no surface regression during the ignition transient, the heat conduction equation reduces to

$$\rho c \frac{\partial T}{\partial t} = k \frac{\partial^2 T}{\partial x^2} \tag{12}$$

The method developed in [17] is reproduced here. By defining the value $\delta(t)$ as the time dependent penetration distance of the thermal wave front, the heat-balance integral can be obtained by multiplying the one-dimensional heat conduction equation by dx, and integrating from 0 to δ,

$$\frac{d}{dt}\left(\theta + T_\infty \delta\right) = \alpha\left[\frac{\partial T}{\partial x}\left(\delta, t\right) - \frac{\partial T}{\partial x}\left(0, t\right)\right] \tag{13}$$

where

$$\theta = \int_0^{\delta(t)} T dx \tag{14}$$

To solve the resulting ordinary differential equation, the temperature profile within the solid propellant is assumed to take a defined form. Typically this is of polynomial form, with a cubic approximation being employed by [24]. In this case the temperature within the solid profile at time t is of the form

$$T = Ax^3 + Bx^2 + Cx + D \tag{15}$$

where A, B, C and D are coefficients that may depend on t. In order to find expressions for the coefficients of the polynomial, boundary and initial conditions are required to close the system of equations.

As the formulation assumes a third-order profile to the polynomial, an additional boundary condition is required to close the system. This is typically taken as

$$\frac{\partial^2 T}{\partial x^2}|_{x=\delta} = 0 \tag{16}$$

This boundary condition is generally referred to as the 'smoothing function' as it has the effect of transitioning the temperature to the ambient conditions smoothly [17]. After a suitable amount of algebraic manipulation of the simultaneous equations, the temperature profile within the solid at time t is determined by

$$T\left(x\right) = \frac{T_s}{\delta^3}\left(\delta - x\right)^3 \tag{17}$$

where the penetration depth δ is given by

$$\delta = \sqrt{12\alpha}\left[\frac{1}{\dot{q}\left(t\right)}\int_0^t \dot{q}\left(t\right) dt\right]^{1/2} \tag{18}$$

By setting $x = 0$, the surface temperature can be obtained,

$$T_s = T_0 + \sqrt{4/3\alpha}\left[\dot{q}\left(t\right)\int_0^t \dot{q}\left(t\right) dt\right]^{1/2} \tag{19}$$

The term $\int_0^t \dot{q}\left(t\right) dt$ can be thought of as the total energy transferred to the propellant from the moment of heat application until time t and is solved via suitable numerical techniques, such as the trapezoidal rule. Propellant ignition is assumed to have occurred when the surface temperature reaches the (experimentally determined) ignition temperature.

3.2 Solution through finite difference approximation

Another approach to solving the one-dimensional heat conduction equation for the solid phase employs the use of a finite difference formulation to resolve the temperature profile within the solid [28]. The simplified one dimensional heat conduction equation is again used, with the same boundary conditions applied. Representing the spatial derivative with a centred finite difference approximation at time n and position i, substituting

$$\frac{\partial^2 T}{\partial x^2} = \frac{T_{i+1}^n - 2T_i^n + T_{i-1}^n}{\triangle x^2} \tag{20}$$

into the solid phase conservation of energy equation gives

$$\frac{\partial T}{\partial t} = \alpha \frac{T_{i+1}^n - 2T_i^n + T_{i-1}^n}{\triangle x^2} \tag{21}$$

The cell temperature at the next time step can then be solved numerically by either a first order Euler approximation, or a more accurate higher order Runge-Kutta method [22]. Using the second-order Runge-Kutta method, the temperature within the solid at the following time step is given by

$$T_i^{n+1} = T_i^n + \triangle t.\mathbf{f}\left(T_i^n + \frac{\triangle t}{2}\mathbf{f}\left(T_i^n\right)\right) \tag{22}$$

where

$$\mathbf{f}\left(T_i^n\right) = \alpha \frac{T_{i+1}^n - 2T_i^n + T_{i-1}^n}{\triangle x^2} \tag{23}$$

By employing appropriate boundary conditions, the temperature profile within the solid can be established by iterating forward in time from the initial temperature distribution, T_∞. Ignition is again established when the surface temperature reaches the ignition temperature.

3.3 Solution through finite difference approximation with surface regression

If the one-dimensional heat conduction equation is extended to include an allowance for the rate of energy convection from the regressing propellant surface, the conservation of energy equation is then reformulated as the standard convection-diffusion equation,

$$\rho c \frac{\partial T}{\partial t} + \rho \dot{r} c \frac{\partial T}{\partial x} = k \frac{\partial^2 T}{\partial x^2} \tag{24}$$

Again the finite difference approach is employed to solve the system of equations. A suitably robust scheme is required, as throughout the ignition transient the problem

can quickly change from diffusion dominated to convection dominated causing significant stability issues [29]. One approach is to use a forward in time centred in space scheme. By using a forward difference in time,

$$\frac{\partial T}{\partial t} = \frac{T_{i+1}^n - T_i^n}{\triangle t} \tag{25}$$

and centered in space,

$$\alpha \frac{\partial^2 T}{\partial x^2} = \alpha \frac{T_{i+1}^n - 2T_i^n + T_{i-1}^n}{\triangle x^2} \tag{26}$$

$$\dot{r} \frac{\partial T}{\partial x} = \dot{r} \frac{T_{i+1}^n - T_{i-1}^n}{2\triangle x} \tag{27}$$

Combining into the original PDE, gives the equation for the forward time step,

$$T_i^{n+1} = T_i^n + \frac{\alpha \triangle t}{\triangle x^2} \left(T_{i+1}^n - 2T_i^n + T_{i-1}^n \right) - \frac{\dot{r} \triangle t}{2\triangle x} \left(T_{i+1}^n - T_{i-1}^n \right) \tag{28}$$

This scheme has been shown to be unreliable in convection dominated problems [29], producing spurious oscillations when

$$\frac{\dot{r} \triangle x}{\alpha} \geq 2 \tag{29}$$

However it is locally stable when the time step is adjusted such that [29]

$$\triangle t \leq \min \left\{ \frac{\triangle x^2}{2\alpha}, \frac{2\alpha}{\dot{r}^2} \right\} \tag{30}$$

A suitable choice for time and space discretisation size that avoids stability issues and solution inaccuracies [29] is given by

$$\triangle t \leq \frac{\triangle x^2}{2\alpha}, \tag{31}$$

where $\triangle x$ also satisfies

$$\triangle x \leq \frac{\alpha}{2\dot{r}} \tag{32}$$

As with the previous models, ignition is considered to have occurred when the surface temperature reaches the ignition temperature.

4 Solid phase ignition model solution technique comparison

In order to develop a greater understanding of the behaviour of the ignition and heat transfer models, a number of synthetic test cases have been developed. Firstly the integral method is compared to the finite difference approximation for a number of heat flux scenarios. A comparison is appropriate, as the same simplifying assumptions are employed in both. Both are solid phase models that neglect the regression of the solid surface. As such it is a comparison of the numerical solution technique, rather than the specific ignition model. This therefore allows direct comparison of the numerical schemes, possibly highlighting any deficiencies in the modelling behaviour. The eight different scenarios, while contrived, will test the models response to heat flux input in a variety of fashions. The first four cases - constant heat flux, ramped heat flux, sinusoidal heat flux and ramped heat flux - do not model the heat transfer within the packed propellant bed. The sinusoidal heat flux and ramped heat flux scenarios have been included to investigate the effect of a varying flux on the temperature profiles.

After the simple solid-phase reaction models are compared, the effect of surface regression rate, $\dot{r}$, on the ignition time of solid propellants is investigated. This is purely a qualitative assessment of the effect of surface regression on the ignition delay of a propellant grain. A range of different values for the regression rate are compared to gauge its importance in the transient ignition process. The propellant properties employed in this study are shown in Table 1.

Initial propellant temperature, T_0	298 K
Constant gas temperature, T_g	2000 K
Propellant density, ρ_s	1577.8 $^{kg}/_{m^3}$
Gas density, ρ_g	1.275 $^{kg}/_{m^3}$
Gas viscosity, μ_g	1.78 $\times 10^{-5}$ Pa $\cdot$ s
Gas ratio of specific heats, γ	1.4
Propellant specific heat capacity, c_p	1550 $^{kJ}/_{kg \cdot K}$
Propellant thermal conductivity, k	0.31 $^{W}/_{m \cdot K}$
Propellant emissivity, ϵ	0.7
Propellant ignition temperature, T_{ign}	400 K

Table 1: *Propellant properties.*

4.1 Finite difference grid spacing sensitivity study

The sensitivity of the numerical solution to the finite difference approximation was investigated to ensure solution independence from spatial discretization. Three grid spacings were investigated, representing coarse, medium and fine grids. Grid spacings of 10 μm,

$1\mu m$ and 0.1 μm were used to investigate the effect on the surface temperature of the propellant under the influence of a constant heat flux. A plot of surface temperature versus time is shown in Figure 2, demonstrating the solutions' dependence on grid spacing. The coarse grid shows a significant deviation from the medium and fine grids. There is minimal difference between the medium and fine grids. By using the medium grid, a significant saving in computing processing time can be achieved, and hence has been used as the grid spacing for the mesh convergence quality assessment.

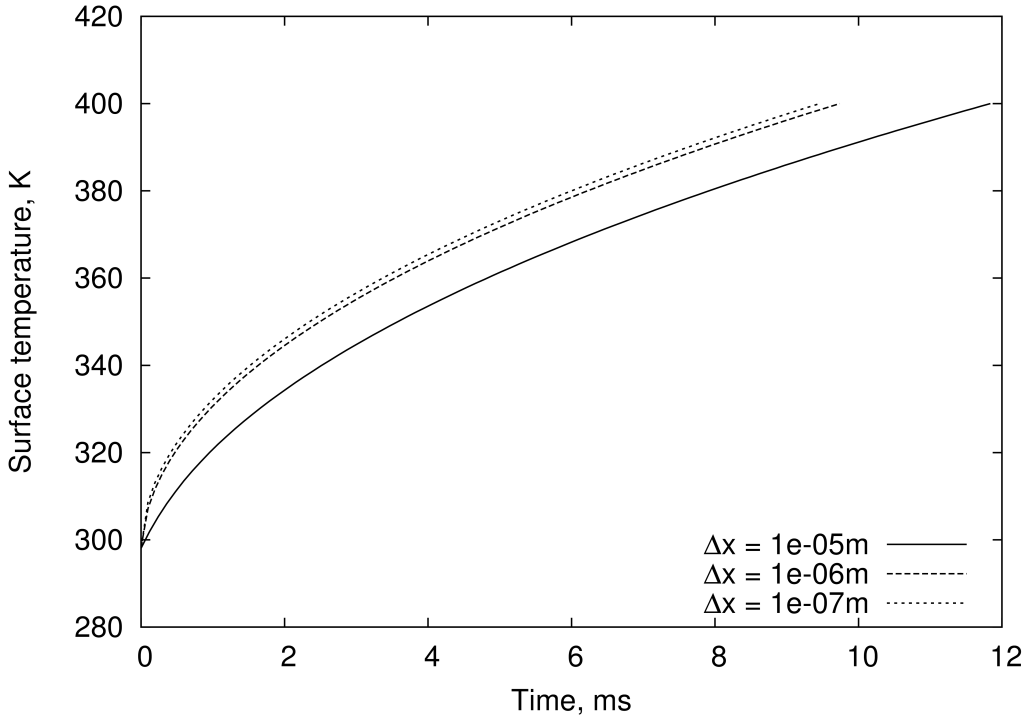

Figure 2: *Surface temperature sensitivity to grid spacing.*

The quality of spatial convergence has been quantified by employing the technique outlined in [30]. By refining the grid by a factor of 2 around the refined mesh ($\Delta x = 1 \times 10^{-06}$m), the order of convergence can be obtained through

$$p = \ln\left(\frac{f_3 - f_2}{f_2 - f_1}\right) / \ln(r)$$

where r is the (constant) refinement ratio and f is the time to ignition at the coarse, medium and fine grid resolutions (subscripts 3, 2 and 1, respectively). By substituting in the values obtained from the numerical simulations, the order of convergence is calculated to be 1.005. This is somewhat low for a second order in space and time scheme. The grid convergence index (CGI) can be calculated as

$$CGI = F_s \frac{(f_2 - f_1)/f_1}{(r^p - 1)}$$

where F_s is a safety factor, taken as 1.25 when three or more mesh spacings are employed. For the medium and fine grids, the grid convergence index is 1.53%.

A temporal discretization study was also performed for both techniques, and it was found that reducing the temporal discretization further from the stability limits provided no additional accuracy to the solution.

4.2 Constant heat flux

The first case investigated involves the comparison of the two numerical techniques under the influence of a constant heat flux. Although this is an unrealistic scenario in practical applications, it allows the comparison of the two techniques with an analytical solution to the heat conduction equation. The heat flux condition at the boundary is given by

$$k\frac{\partial T}{\partial x}|_{x=0} = \dot{q} \tag{33}$$

where $\dot{q}$ is a constant. The propellant is assumed to have ignited when the surface temperature reaches T_{ign} =400K. The analytical solution is given as [17]

$$T_s = T_0 + \sqrt{4/\pi\alpha t} \cdot \dot{q} \tag{34}$$

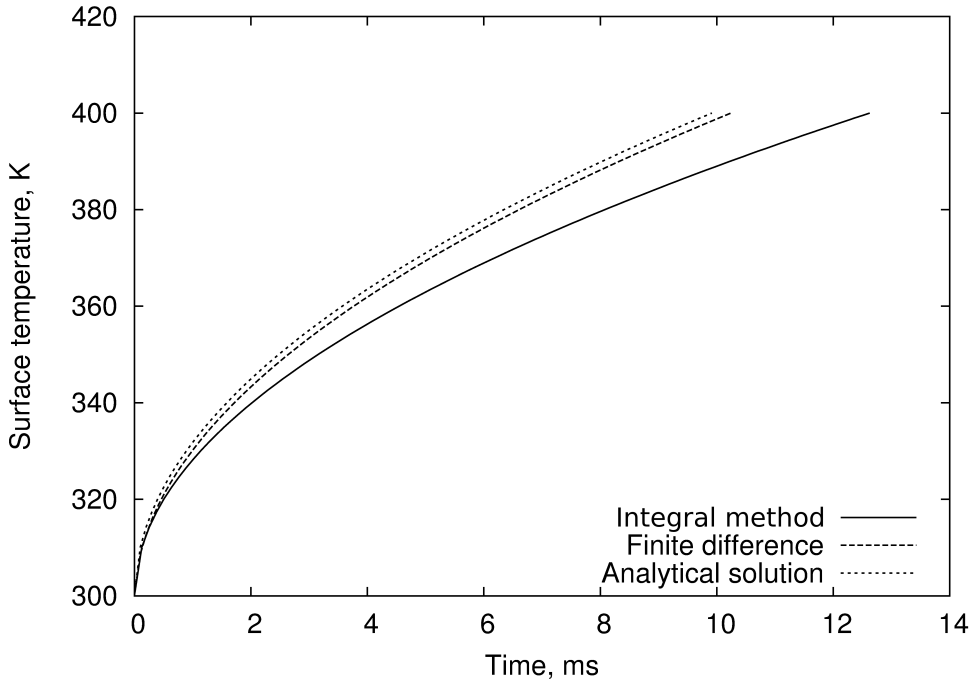

Figure 3: *Surface temperature time history, constant heat flux.*

Figure 3 shows a plot of the solid propellant surface temperature. The plot shows that the finite difference solution is able to closely match the analytical solution, while

the integral method diverges from the actual solution as time progresses. The cause for this can be seen by comparing the integral method cubic approximation (Eq. 19) and the analytical solution (Eq. 34). They differ by approximately 2.3% at each time step, which increases the absolute error as time progresses.

4.3 Constant heat transfer coefficient

The second case investigates the individual models' response to a temperature dependent heat flux at the boundary, such that

$$k\frac{\partial T}{\partial x}|_{x=0} = h\left(T_g - T_s(t)\right) \tag{35}$$

where h and T_g are held constant. The propellants are assumed to have ignited when the surface temperature reaches 400 K. The results of the comparison between the cubic approximation and the finite difference formulation are shown in Figure 5. It can be seen that both curves have the same general form, however the finite difference approximation rises to the ignition temperature faster than the cubic approximation.

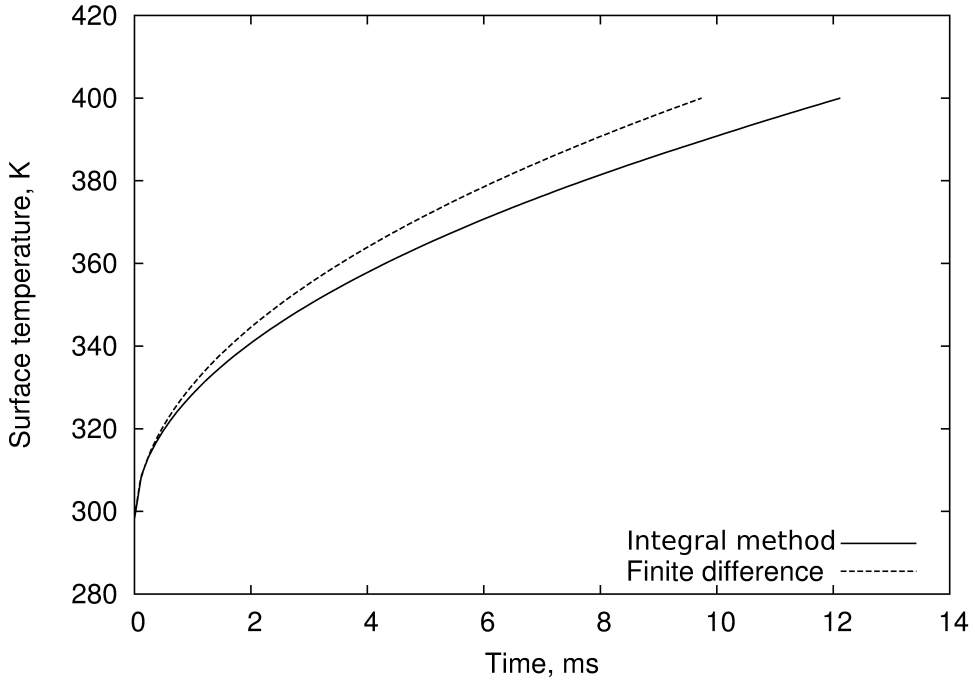

Figure 4: *Surface temperature time history, temperature dependent heat flux.*

4.4 Ramped heat heat transfer coefficient

The third case investigates a time-dependant linear increase in heat transfer coefficient, such that

$$k\frac{\partial T}{\partial x}|_{x=0} = h\left(T_g - T_s(t)\right) \tag{36}$$

where

$$h = f\left(t\right) = \dot{h}_{const} \cdot t \tag{37}$$

The results for both the cubic approximation and the finite difference formulation are shown in Figure 5.

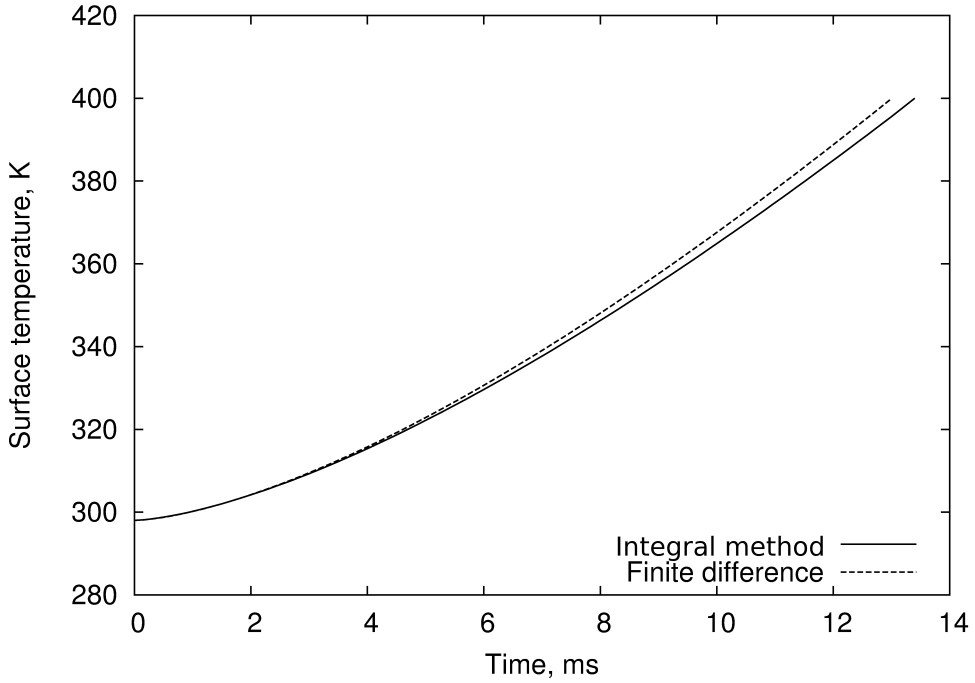

Figure 5: *Surface temperature time history, ramped heat flux.*

The two approximations appear to give similar results for the ignition time. As in the previous two cases, the finite difference approximation reaches the ignition temperature at a faster rate than the cubic approximation, however the lag is significantly reduced.

4.5 Varying heat transfer coefficient

The fourth case investigated is that of a varying heat flux coefficient with a constant gas temperature. This case was devised in order to scrutinise the behaviour of the cubic approximation against varying heat flux. The boundary condition is therefore given as

$$k\frac{\partial T}{\partial x}|_{x=0} = h\left(T_g - T_s(t)\right) \tag{38}$$

where

$$h = f(t) = h_{const} + \frac{h_{const} \sin(\pi t/180s)}{2} \tag{39}$$

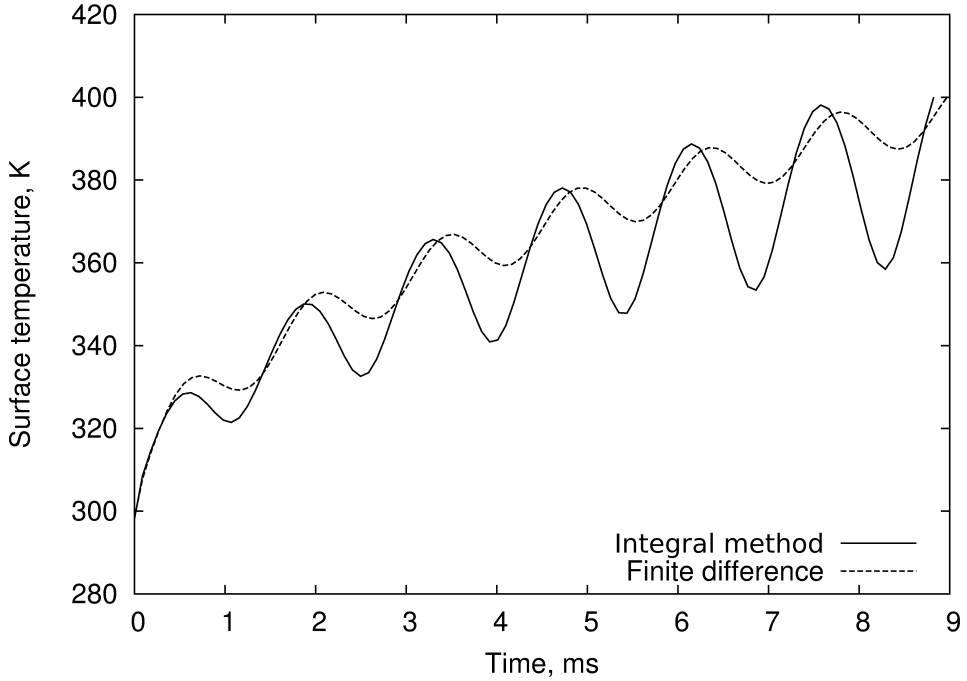

Figure 6: *Surface temperature time history, varying heat flux.*

A plot of propellant surface temperature against time shows the results from the two approximations in Figure 6. In this case it is apparent that the integral method gives a faster ignition time than the finite difference approximation. The integral method is more sensitive to the sinusoidal heat flux, which can be seen in the greater amplitude of the oscillations about the average temperature increase. The integral method works by assuming a temperature profile within the solid, based only on the thermal properties of the material, the instantaneous heat flux and the internal energy of the solid. It does not, therefore, allow for the lag of the thermal wave within the solid due to a decrease in incident heat flux. This is an obvious shortcoming of the method, but the final results are not significantly affected in this case, with the ignition time decreased by 0.1 ms.

From Figure 6 it is clear that the difference in the ignition time between the two methods is dependant on the choice of T_{ign}. This could present an issue, as at times the two methods may differ by up to 0.3 ms. Another point that should be noted is the difference in the peak value of the oscillations for the solution as time progresses. This implies that for some ignition temperatures, one method may indicate the propellant is ignited while the other method lags until the next heat flux wave peak. This could result in significantly different ignition time estimations between the two methods.

4.6 Step function heat transfer coefficient

To further test the response of both methods to highly variable heat fluxes, a step function heat flux profile was employed. By inspection of the surface temperature profile equation obtained from the integral method, the surface temperature will be equal to the initial temperature when the instantaneous heat flux is zero. It is therefore obvious that an incorrect surface temperature will result when the heat flux is zero. It is of interest however to see if the method is able to recover to the correct surface temperature when the heat flux is reapplied based on the total internal energy of the propellant. The heat flux boundary condition is given as

$$k\frac{\partial T}{\partial x}|_{x=0} = h\left(T_g - T_s(t)\right) \tag{40}$$

where

$$h = f\left(t\right) = h_{constant} \cdot \mho\left(t\right); \qquad \mho\left(t\right) = \begin{cases} 0 & 0 < t \leq 0.5ms \\ 1 & 0.5 < t \leq 1.0ms \\ 0 & 1.0 < t \leq 1.5ms \\ \ldots & etc \end{cases} \tag{41}$$

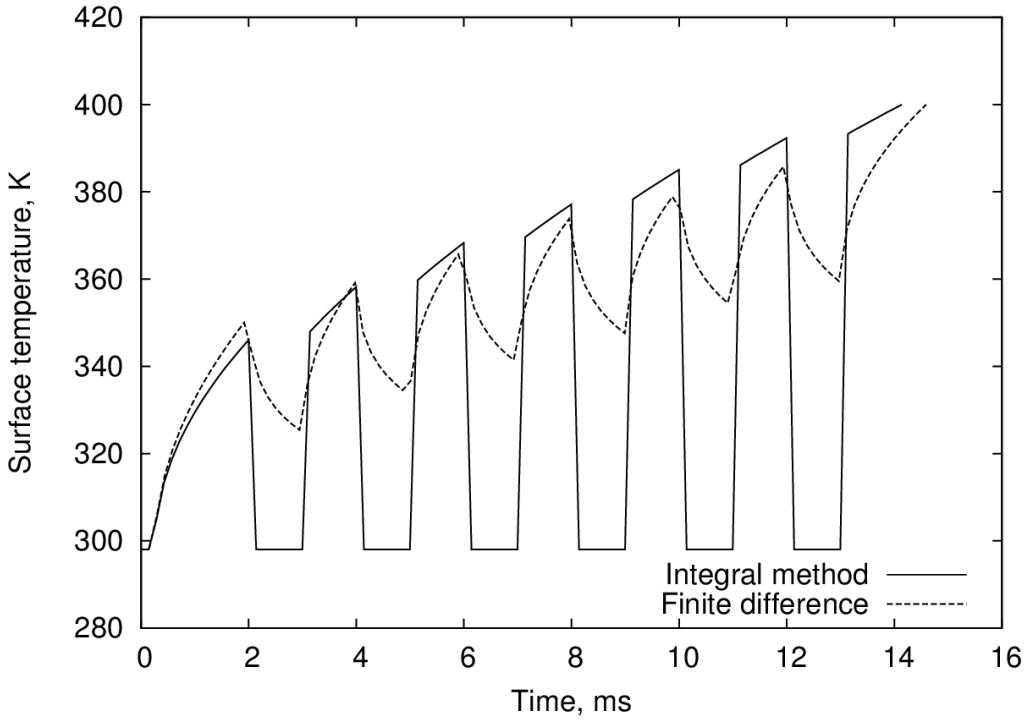

Figure 7: *Surface temperature time history, step function heat flux.*

The results from the simulations are shown in Figure 7. The finite difference approximation shows an initial increase in surface temperature, which decreases slowly when the

heat flux is switched off. As the finite difference technique solves the temperature profile within the solid, heat diffusion away from the surface can be calculated. The behaviour of the integral method to this (quite contrived) heat flux is significantly different. The two methods follow a very similar profile upon the initial application of heat, but when the flux is switched off the surface temperature approximated by the integral method drops immediately to zero. Upon the re-application of heat, the surface temperature given by the cubic approximation jumps up to its previous position. The temperature profile within the solid is derived from the stored internal energy within the solid, and the instantaneous heat flux to the surface. The integral method over-estimates surface temperature at this point (as compared to the finite difference equation), which is attributed to the assumption of a cubic profile no longer being valid. While there is no heat flux to the solid propellant surface, heat is still conducted away from the hot solid regions to cooler regions further from the propellant surface. The temperature profile is therefore no longer cubic, and a key assumption for the formulation of the cubic approximation is no longer valid. The cubic approximation gets further away from the finite difference approximation as the number of flux intervals increases. For the specified T_{ign}, by chance, the final ignition time predicted by the two methods is very similar.

4.7 Packed bed heat transfer coefficient, varying velocity and constant temperature

The next step in the analysis involved implementation of a packed bed heat transfer approximation. This was done in order to assess both models' behaviour under the application of more complex and realistic heat flux scenarios. The heat transfer is a function of a number of physical processes all acting to transfer heat energy to the solid propellant. Due to the complexity of the heat transfer mechanisms present, no one complete method exists that accurately accounts for all processes. Rather, empirical formulations are typically used to approximate the amount of heat transferred to (and from) the solid propellant and the surroundings. This section outlines some of the models that have been previously used in interior ballistic and propellant combustion modelling, with the aims of selecting the most suitable model for use in Casbar.

Gough [31] employs an empirical approximation to the heat transfer, assuming radiative and convective mechanisms, based on fluidized bed theory [32]. The heat transferred to the solid propellant grain is a function of temperature and is given by

$$\dot{q} = (h_{conv} + h_{rad})\,(T_g - T_s) \tag{42}$$

The convective and radiative film coefficients are determined by

$$h_{rad} = \epsilon\sigma\,(T_g + T_s)\left(T_g^2 + T_s^2\right) \tag{43}$$

and

$$h_{conv} = \frac{\mathrm{Nu} \cdot k_f}{D_p} \tag{44}$$

In the above expressions ϵ is the emissivity of the propellant/gas interface, σ is the Stefan Boltzmann constant, Nu is the Nusselt number, k_f is the thermal conductivity of the gas evaluated at the film temperature and D_p is the effective grain diameter, which is given by

$$D_p = \frac{6V_p}{S_p} \tag{45}$$

The Nusselt number is determined by

$$Nu = 0.4Pr^{1/3}Re_s^{2/3} \tag{46}$$

where

$$Re_s = \rho_f|\overrightarrow{u_g} - \overrightarrow{u_s}|D_p/\mu_f \tag{47}$$

and

$$Pr = \frac{c_s\mu_f}{k_f} \tag{48}$$

In the above expression μ_f and k_f are the viscosity and thermal conductivity of the gas evaluated at the film temperature and c_s is the specific heat capacity of the solid phase. Lowe [22] also employs an empirical approximation for the heat transfer, however the heat transfer is assumed to occur only through radiation and conduction, with convective effects neglected. This inaccuracy is acknowledged, with experiments highlighting the need for a scaling factor to be introduced to obtained realistic solid temperature profiles. Identical to [31], the heat flux due to radiation is given by

$$\dot{q}_{rad} = \sigma\epsilon\left(T_g^4 - T_s^4\right) \tag{49}$$

The conductive heat transfer differs however, and is given by the empirical relation

$$\dot{q}_{cond} = k_f c_s T^{0.25}\frac{\dot{r}^{0.8}}{D_p^{0.2}}\left(T_g - T_s\right) \tag{50}$$

No details as to the origin or background theory of this expression were provided in [22].

Both of the above approaches to modelling the heat transfer within the packed propellant bed neglect all mechanisms besides convective and radiative heating. Unfortunately this approach neglects the heat transfer due to non-gaseous igniter products. These products can form a significant portion of the igniter gases, and as such the heat transfer can be under predicted. Particle-particle interaction models can be employed to model this aspect of heat transfer [33], however this approach is not currently being pursued within the Casbar framework.

The first numerical simulation involved examining the behaviour under the influence of a varying gas velocity, with a constant gas temperature. The heat flux boundary condition is therefore

$$k\frac{\partial T}{\partial x}|_{x=0} = h\left(T_g - T_s(t)\right) \tag{51}$$

where

$$h = h_{conv} + h_{rad} \tag{52}$$

and

$$h_{conv} = \frac{Nuk}{D_p} \tag{53}$$

$$h_{rad} = \epsilon\sigma\left(T_g + T_s\right)\left(T_g^2 + T_s^2\right) \tag{54}$$

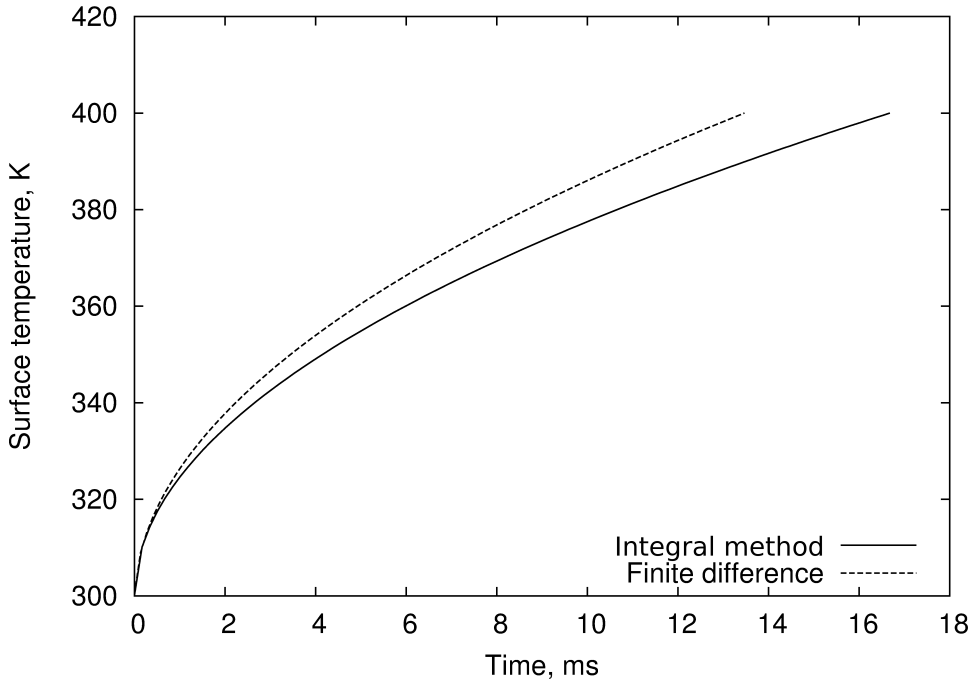

Figure 8: *Surface temperature time history, packed bed heat transfer approximation with varying velocity.*

The results shown in Figure 8 indicate that by varying the gas velocity, little influence is made on the surface temperature of the propellants calculated by the two methods. This is simply because convective heat transfer plays a much less significant role in the propellant ignition case being analysed.

4.8 Packed bed heat transfer coefficient, constant velocity and varying temperature

The final case being examined is again using the packed bed heat transfer approximations, however this time with a varying gas temperature. In this test case, the gas temperature is varied by a sinusoidal function, giving oscillations about a defined mean temperature. As radiation plays a much more significant role in the heat transfer to the solid propellant at high temperatures due to the quartic dependency, both approximations will be significantly tested by this condition.

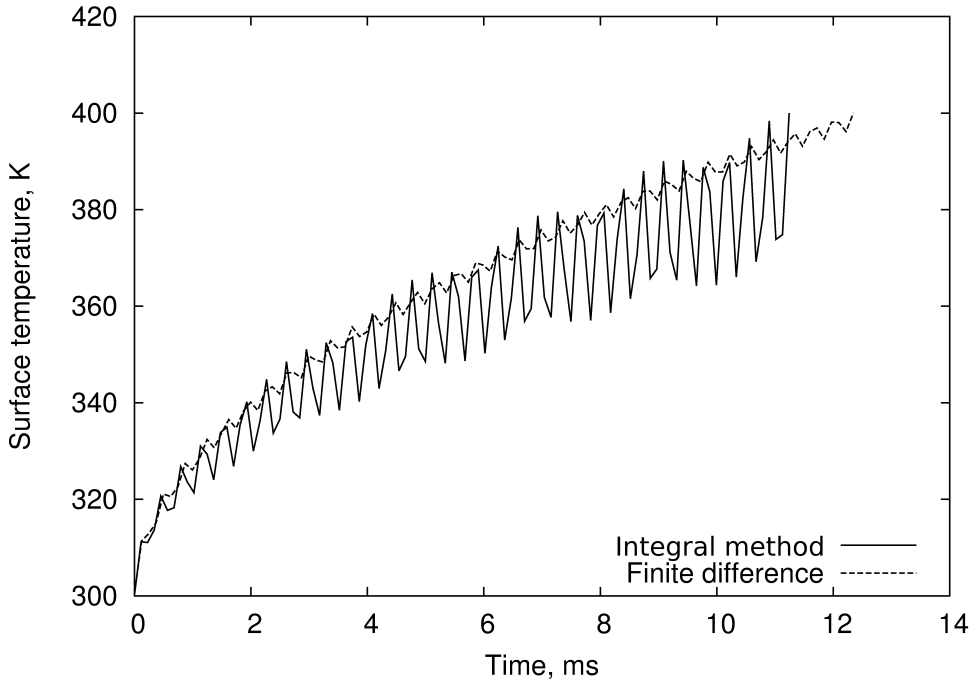

Figure 9: *Surface temperature time history, packed bed heat transfer approximation with varying gas temperature.*

Figure 9 shows the response of the two models to the applied heat flux. It can be clearly seen that the integral is significantly affected by the varying heat flux. This is again due to the sensitivity of the method to the instantaneous heat flux. The final ignition times determined by both methods does not vary significantly between the two methods.

4.9 Effect of surface regression on ignition time

To understand the effect of surface regression on the ignition time of the propellant, the finite difference case discussed in Section 3.3 with surface regression has been investigated. Figure 10 shows surface temperature history plots for various values of $\dot{r}$, as well as the original non-regressing case. As the regression rate increases, the time to ignition of the solid propellant also increases. This can be attributed to the convection term within the energy equation.

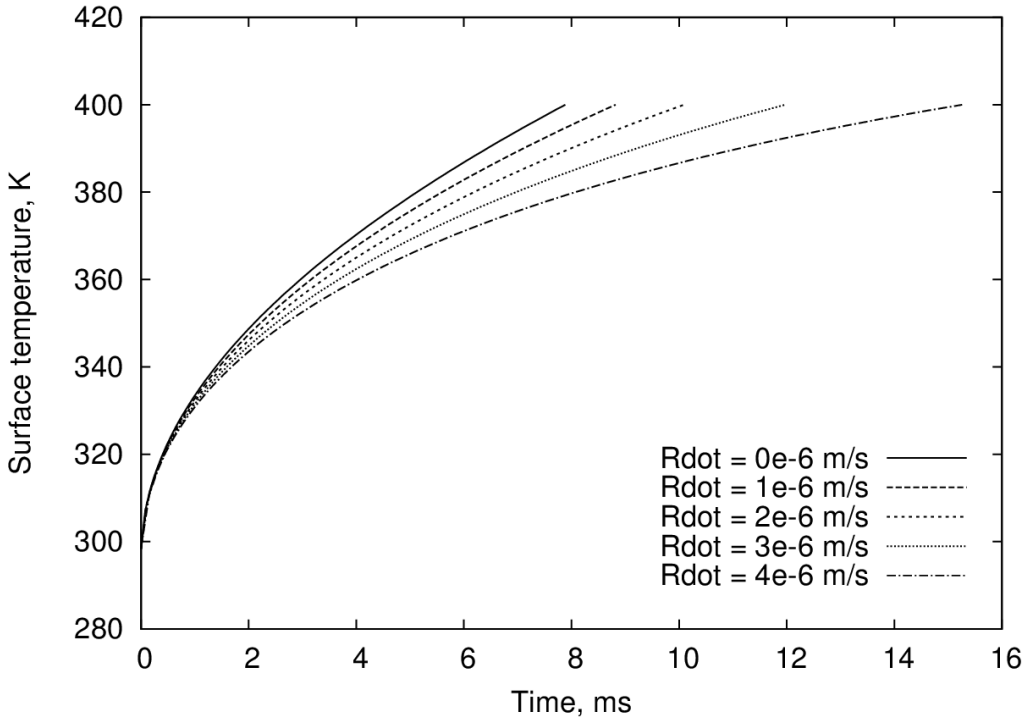

Figure 10: *Effect of varying regression rate on propellant ignition time.*

4.10 Numerical scheme performance comparison

A comparison of the integral and finite difference methods for the propellant ignition problem was performed on the constant heat transfer scenario. As this is the simplest heat transfer problem, it will provide somewhat of a 'best case scenario' in terms of computational efficiency. This calculation, which can be considered typical for a solid propellant ignition calculation within Casbar, would highlight the efficiency differences of the two methods. Both numerical schemes were employed with the same initial and boundary conditions, with the processing time recorded. For the integral method, a single calculation of the surface temperature would take 0.574 ms, as opposed to 2.69 ms for the finite difference approach. This represents a four-fold increase in the computational expense of the finite difference method over the integral method based on calculation time alone. Considering that this calculation is required to be performed in each individual cell at every time step, a significant computational penalty is associated with employing the finite difference approach.

5 Summary and conclusion

A wide range of approaches to solid propellant ignition modelling are available. The physical process of ignition and combustion in solid propellants is complex and case-dependant,

and as such no single model can be considered appropriate for every problem. Simplifications are required, which may or may not be applicable for different scenarios. The three main areas of ignition models (solid-phase, heterogeneous and gas-phase reactions models) encompass a broad range of complexity and numerical efficiency. It is therefore desirable to choose a model that is accurate, while being flexible for a wide range of possible scenarios for implementation into Casbar.

In Casbar it is required that the interior ballistic propellant ignition model is adequately robust, while reducing the impact on the simulation time. In all of the investigated heat flux scenarios, the integral method was able to adequately approximate the final ignition time to within an acceptable level of accuracy (in comparison to the finite difference approximation). Situations involving highly variable heat fluxes were employed to test the applicability of the integral method. These scenarios were constructed to accentuate the variability of the heat flux, and situations like this are not expected in typical interior ballistic simulations. The integral method is therefore considered an appropriate candidate for implementation in Casbar.

References

1. W.A. Rosser, N. Fishman, and H. Wise. Ignition of simulated propellants based on ammonium perchlorate. Technical report, Stanford Research Institute, 1965.

2. L. Deluca, T.J. Ohlemiller, L.H. Caveny, and M. Summerfield. Solid propellant ignition and other unsteady combustion phenomena induced by radiation. Technical report, Princeton University, 1976.

3. RJ. Gollan, BT. O'Flaherty, PA. Jacobs, and IA. Johnston. *Casbar user's guide.* Defence Science and Technology Organisation, November 2009.

4. M.W. Beckstead, K. Puduppakkam, P. Thakre, and V. Yang. Modeling of combustion and ignition of solid-propellant ingredients. *Progress in Energy and Combustion Science*, 33:498–551, 2007.

5. N. Kubota. Survey of rocket propellants and their combustion characteristics. *Fundamentals of Solid-Propellant Combustion*, 1:1–26, 1984.

6. F. Peugeot, S. Peters, H. Gokee, I. Maxey, I. Martin, D. Stalker, J. Petherbridge, G. Roach, P. Henning, P. Lee, B. Isle, and M. Esteban. Im issues related to gun propelling charges design. Technical report, Munitions Safety Information Analysis Centre, 2004.

7. N. Kubota. *Propellants and explosives: Thermochemical aspects of combustion.* Wiley-VCH, 2002.

8. M.S. Miller and W.R. Anderson. Cyclops, a breakthrough code to predict solid-propellant burning rates. Technical report, Army Research Laboratory, 2003.

9. M.L. Gross. *Two-dimensional modeling of AP/HTPB utilizing a vorticity formulation and one-dimensional modeling of AP and ADN.* PhD thesis, Brigham Yound University, 2007.

10. M.S. Miller. Burning-rate models and their successors: A personal perspective. Technical report, Weapons and Materials Research Directorate, ARL, 2003.

11. M.S. Miller. In search of an idealized model of homogeneous solid propellant combustion. *Combustion and Flame*, 46:51–73, 1982.

12. B.L. Hicks. Theory of ignition considered as a thermal reaction. *The Journal of Chemical Physics*, 22:414–429, 1954.

13. C.E. Hermance. *Fundamentals of Solid-propellant Combustion*, chapter Solid-propellant ignition theories and experiments, pages 239–258. American Institute of Aeronautics and Astronautics, 1984.

14. E.W. Price, H.H. Bradley Jr, G.L. Dehority, and M.M. Ibiricu. Theory of ignition of solid propellants. *AIAA Journal*, 4:1153–1181, 1966.

15. A.D. Baer and N.W. Ryan. An approximate but complete model for the ignition response of solid propellants. *AIAA Journal*, 6:872–877, 1968.

16. A. Peretz, K.K. Kuo, L.H. Caveny, and M. Summerfield. Starting transient of solid-propellant rocket motors with high internal gas velocities. *AIAA Journal*, 11:1719–1727, 1973.

17. T.R. Goodman. Application of integral methods to transient non-linear heat transfer. *Advances in Heat Transfer*, 1:51–122, 1964.

18. R. Anderson, R.S. Brown, G.T. Thompson, and R.W. Ebeling. Theory of hypergolic ignition of solid propellants. *AIAA reprint*, 1963.

19. H.H. Bradley Jr. A unified theory of solid propellant ignition. part 1 - development of mathematical model. Technical report, Naval Weapons Center, China Lake, California, 1974.

20. F.A. Williams. Theory of propellant ignition by heterogeneous reaction. *AIAA*, 4:1354–1357, 1966.

21. Y.C. Liau. *A comprehensive analysis of RDX propellant combustion and ignition with two-phase subsurface reactions.* PhD thesis, Pennsylvania State University, 1996.

22. C. Lowe. *CFD modelling of solid propellant ignition.* PhD thesis, Cranfield University, 1996.

23. M.S. Miller. Thermophysical properties of six solid gun propellants. Technical report, Army Research Laboratory, 1997.

24. P.S. Gough. Two-dimensional, two-phase modeling of multi-increment bagged artillery charges. Technical report, US Army Ballistic Research Laboratory, 1983.

25. C. Boulnois, C. Strozzi, A. Bouchama, and P. Gillard. A numerical tool for evaluating solid propellant ignition models. In *26th International Symposium on Ballistics*, 2011.

26. H. Miura, A. Matsuo, and Y. Nakamura. Investigation on ignition and combustion process in granular solid propellant chamber. In *26th International Symposium on Ballistics*, 2011.

27. M.J. Nusca. Multidimensional interior ballistics modeling with extensions to igniter design and operation. In *26th International Symposium on Ballistics*, 2011.

28. A.F. Mills. *Heat Transfer.* Prentice Hall, 1999.

29. J. Noye. Numerical methods for solving the transport equation. In *Numerical Modelling: Applications to Marine Systems.* Elsevier, 1987.

30. J.W. Slater, J.C. Dudek, and K.E. Tatum. The nparc alliance verification and validation archive. Technical report, National Aeronautical and Space Administration, 2000.

31. P.S. Gough. The xnovaktc code. Technical report, U.S. Army Laboratory Command, 1990.

32. N.I. Gelperin and V.G. Einstein. *Heat transfer in fluidized beds.* Academic Press, 1971.

33. C. Woodley. Modelling the effects of non-gaseous igniter combustion products on the ignition of gun propellants. In *26th International Symposium on Ballistics*, 2011.

DEFENCE SCIENCE AND TECHNOLOGY ORGANISATION DOCUMENT CONTROL DATA	1. CAVEAT/PRIVACY MARKING

2. TITLE	3. SECURITY CLASSIFICATION
Review of Solid Propellant Ignition Models Relative to the Interior Ballistic Modelling of Gun Systems	Document (U) Title (U) Abstract (U)
4. AUTHORS	5. CORPORATE AUTHOR
A. Harrland and I.A. Johnston	Defence Science and Technology Organisation PO Box 1500 Edinburgh, South Australia 5111, Australia

6a. DSTO NUMBER	6b. AR NUMBER	6c. TYPE OF REPORT	7. DOCUMENT DATE
DSTO–TR–2735	015-373	Technical Report	August, 2012

8. FILE NUMBER	9. TASK NUMBER	10. TASK SPONSOR	11. No. OF PAGES	12. No. OF REFS
2012/1083891/1	LRR 07/249	DSTO	34	33

13. URL OF ELECTRONIC VERSION	14. RELEASE AUTHORITY
`http://www.dsto.defence.gov.au/publications/scientific.php`	Chief, Weapons Systems Division

15. SECONDARY RELEASE STATEMENT OF THIS DOCUMENT

Approved for Public Release

OVERSEAS ENQUIRIES OUTSIDE STATED LIMITATIONS SHOULD BE REFERRED THROUGH DOCUMENT EXCHANGE, PO BOX 1500, EDINBURGH, SOUTH AUSTRALIA 5111

16. DELIBERATE ANNOUNCEMENT

No Limitations

17. CITATION IN OTHER DOCUMENTS

No Limitations

18. DSTO RESEARCH LIBRARY THESAURUS

Solid propellants	Ballistics
Ammunition	Ignition
Computational fluid dynamics	Numerical methods

19. ABSTRACT

The modelling of solid propellant ignition is investigated with the aim of implementation into the numerical code Casbar. The current state of the art in solid propellant ignition and combustion modelling is reviewed, with a simplified condensed phase ignition model chosen as the suitable candidate. A number of methods of solving the mathematical models are analysed, with results compared. Based on these results, the solution by integral methods to the condensed phase model was chosen for implementation into Casbar.